Morphology and Organization of Phospholipid/Diacetylene Langmuir Films Studied by Brewster Angle Microscopy and Fluorescence Microscopy

ARTICLE *in* THE JOURNAL OF PHYSICAL CHEMISTRY B · SEPTEMBER 2002

Impact Factor: 3.3 · DOI: 10.1021/jp020393j

4 AUTHORS, INCLUDING:

Amir Berman
Ben-Gurion University of the Negev
53 PUBLICATIONS **1,708** CITATIONS

SEE PROFILE

Morphology and Organization of Phospholipid/Diacetylene Langmuir Films Studied by Brewster Angle Microscopy and Fluorescence Microscopy

R. Volinsky,[†] F. Gaboriaud,[†,‡] A. Berman,*[,§] and R. Jelinek*[,†]

Ilse Katz Center for Nano- and Mesoscience and Technology, and Department of Chemistry and Department of Biotechnology Engineering, Ben Gurion University of the Negev, Beersheva 84105, Israel

Received: February 11, 2002

The thermodynamic and morphological properties of binary films of phospholipids and diacetylene lipids deposited at the air−water interface have been studied. Brewster angle microscopy (BAM) and fluorescence microscopy have been applied to investigate the formation, organization, and structure of the film domains. BAM data acquired at different temperatures, film compositions, and surface pressures reveal the appearance of distinct patterns of the diacetylenic moieties. In particular, the exceptionally high-quality BAM images point to dendritic and fractal-like appearance of the diacetylene domains; these phenomena are discussed in a framework of diffusion-limited aggregation processes. The results of the microscopy analyses further indicate that the two molecular components already segregate at low compression pressures and that the combined effects of film composition and temperature influence the occurrence of transitions between different phases within the films. This study sheds light on the molecular and cooperative features of mixed lipid/diacetylene films and further helps to understand the unique biosensing properties of these assemblies.

Introduction

Diacetylenic lipids, first synthesized by Wegner in 1969,[1] have attracted considerable interest due to the unique chromatic properties of their polymerized form, polydiacetylene or PDA.[1] Applications of PDAs in various fields have been explored, including molecular electronics,[2] optical waveguides,[3] and chromatic biosensors.[4] We have recently demonstrated that mixed assemblies of lipids and PDA can be utilized as colorimetric sensors for studying a variety of biochemical phenomena, such as peptide−membrane interactions,[5] ion transport,[6] antibody−epitope recognition,[7] and others.[8,9] These studies indicate that the lipid/polydiacetylene surface essentially serves as a platform for interfacial biological processes. To realize the full biochemical and biotechnological potential of the lipid/PDA system, a comprehensive understanding of the organization and molecular interactions in these assemblies is essential. Lipid/PDA aggregates have been mainly studied in vesicle organization.[10] Recently, we have reported on a study of the organization and chromatic properties of phospholipid/diacetylenic lipids Langmuir−Schaefer [LS] mixed films.[11]

In this work, we present a detailed study of the growth, morphologies, and organization of mixed Langmuir films at the air−water interface, composed of natural membrane phospholipids (dimyristoylphosphatidylcholine, DMPC) and the synthetic diacetylene fatty acid tricosadyinoic acid (TRCDA), utilizing Brewster angle microscopy (BAM) and fluorescence microscopy. The experiments have been designed to investigate the microstructures, domain formation, and molecular spatial distribution within the films. An important goal of this work has been to evaluate the effects of various physical parameters, such as temperature, film composition, and surface pressure, upon the structural properties of the mixed assemblies. Elucidation of the interplay between the two film components is particularly important for gaining a thorough understanding of the chromatic transitions in the PDA matrix induced by biological processes occurring exclusively at the lipid domains.

Brewster angle microscopy has been the primary analytical technique employed in this study. BAM is a relatively new surface technique based on the zero reflectance of a p-polarized light from a surface at the Brewster's angle of incidence, thus enabling a visual inspection of various molecular phenomena on surfaces, including ordering, nucleation, and domain growth.[12,13] BAM is expected to be particularly informative for studying PDA interfaces because of the differences between the indexes of refraction of the compressed diacetylene domains and both the water subphase and the phospholipids in the mixed phospholipid/TRCDA films.[11] A recent BAM study has explored structural and topographical issues pertaining to PDA films.[14,15]

Experimental Section

Materials and Film Preparation. The monomeric diacetylene 10,12-tricosadiynoic acid (TRCDA) was purchased from GFS Chemicals (Powell, OH). The compound was further purified by dissolving the solid in chloroform ($CHCl_3$) and filtering through a 0.45 μm Nylon filter. The purified solid was obtained by evaporation of the solvent. Dimyristoylphosphatidylcholine (DMPC) (Avanti Polar Lipids, Alabaster, AL) was used as received.

The DMPC and TRCDA were dissolved in chloroform at a concentration of 2 mM. The various molar fractions were prepared by mixing the appropriate volumes of parent solutions of each compound. The water subphase used in the Langmuir trough was doubly purified by a Barnstead D7382 water purification system (Millipore), producing distilled water having 18.3 mΩ resistance.

* To whom correspondence should be addressed. E-mail addresses: razj@bgumail.bgu.ac.il and aberman@bgumail.bgu.ac.il.
[†] Department of Chemistry.
[‡] Present Address: Laboratoire de Chimie Physique et Microbiologie pour l'Environnement, UMR 7564, CNRS, UHP-Nancy 1, 405 rue de Vandoeuvre, F-54600 Villers-lès-Nancy, France.
[§] Department of Biotechnology Engineering.

10.1021/jp020393j CCC: $22.00
Published on Web 08/14/2002

The fluorescent probe, *N*-(7-nitrobenz-2-oxa-1,3-diazol-4-yl)-1,2-dihexadecanoyl-*sn*-glycero-3-phosphoethanolamine, triethylammonium salt (NBD-PE) was purchased from Molecular Probes, Inc. (Eugene, Oregon) in HPLC grade purity and was used as received. The probe was dissolved in chloroform at a concentration of 0.5 mM and was added to TRCDA/DMPC solutions at a concentration of 2 mol %.

Surface Pressure−Area Isotherms. All surface pressure−area isotherms were measured with a computerized Langmuir trough manufactured by NIMA (model 622/D1 (7×50 cm^2) Nima technology Ltd, Coventry, U.K.). The experiments were carried out at different temperatures using a thermostated Teflon barostat. The surface pressure was monitored using a 1-cm-wide filter paper as a Wilhelmy plate. For each isotherm experiment, 25 μL of the solution was spread on the water subphase (measured pH of 6.3). Compression started after solvent evaporation (15 min) and was carried out at a constant barrier speed of 3.3 Å^2 molecule^{-1} min^{-1}. The surface pressure measurements were repeated at least three times, using a fresh mixture in each experiment. The isotherms presented are the average of the three experimental runs, which were reproducible within the error area of $\pm$0.6 Å^2 molecule^{-1}.

Brewster Angle Microscopy. A NFT (Gottingen, Germany) Brewster angle microscope mounted on a Langmuir film balance was used to observe the microscopic structures in situ. The light source of the BAM was a frequency doubled Nd:YAG laser with a wavelength of 532 nm and 20−70 mW primary output power in a collimated beam. The BAM images were recorded with a CCD camera. The scanner objective was a Nikon super-long working distance objective with a nominal 10× magnification and diffraction limited lateral resolution of 2 μm. The images were corrected to eliminate side ratio distortion originating from a nonperpendicular line of vision of the microscope.

Fluorescence Microscopy. Samples for the fluorescence microscopy experiments were transferred onto octadecyltriethoxysilane (OTS)-modified glass surfaces, following polymerization on the water subphase. Glass slides were dipped in a cleaning (piranha) solution consisting of 70 mL of H_2SO_4 and 30 mL of H_2O_2 for 30 min at 70 °C, which was followed by sonication in the same solution for 10 min. Following the cleaning, the glass was rinsed thoroughly with pure water and dried at 70 °C. To form the self-assembled monolayers on the surface, the glass was immersed in a solution of 300 μL of OTS in 100 mL of cyclohexane for 12 h. Glass slides were then rinsed with cyclohexane to remove noncovalently bound OTS molecules. The polymerized films were transferred to the modified glass slides by a horizontal touch method (Langmuir−Schaefer method).[16,17] Fluorescence microscopy measurements were carried out on an Olympus ix 70 microscope equipped with a Cohu 4910 digital camera. The experiments employed a narrow-band filter cube U-MNIBA 2, excitation 470−490 nm, beam splitter 505 nm, outgoing filter 510 to >550 nm. Images were processed with "Scion image" software and presented as the 50-frames integration result.

Results and Discussion

A previous thermodynamic and microscopic analysis of TRCDA films at the air−water interface has determined that compressed diacetylene acid undergoes distinct temperature-dependent phase transitions.[11] Figure 1 depicts surface pressure−area isotherms recorded at 2 °C temperature intervals around 18 °C, in which a unique thermodynamic profile of TRCDA was previously observed.[11] The isotherms clearly demonstrate the existence of different compression profiles and phase

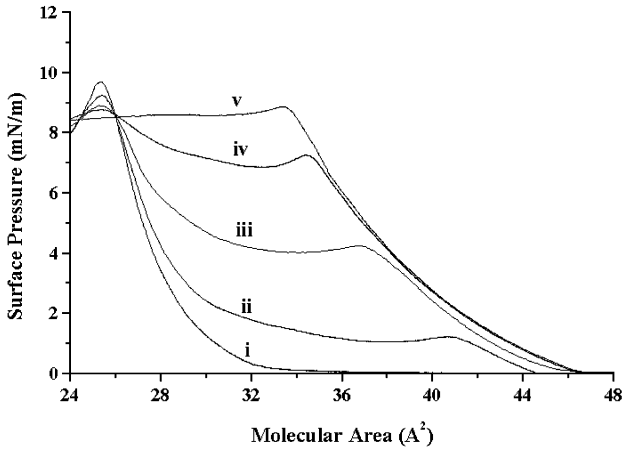

Figure 1. Surface pressure−area isotherms of TRCDA at different temperatures: (i) 14; (ii) 16; (iii) 18; (iv) 20; (v) 22 °C.

formation around that temperature. Specifically, at temperatures close to 18 °C, Figure 1ii−iv, an incipient liquid-expanded phase is detected, which transforms into a condensed phase at progressively higher pressures as the temperature is increased. A plateau region of coexisting expanded and condensed phase follows, consistent with the first-order nature of the expanded−condensed transition.[18] The situation is different at temperatures farther away from 18 °C. At 14 °C, for example (Figure 1i), a condensed phase initially forms prior to the collapse pressure. At 22 °C (Figure 1v), on the other hand, no condensed phase is observed because the higher temperature destabilizes the crystallization of the condensed TRCDA phase. This essentially results in the presence of liquid expanded domains up to the collapse pressure after which an equilibrium exists between a multilayered film and an expanded phase.[11]

BAM analysis provides a wealth of microscopic information upon the compression processes, as well as illuminates the growth phenomena and domain formation within TRCDA films. Figures 2−4 present BAM images acquired at different temperatures and surface pressures. The BAM data reveal the appearance and transformation of distinct structures at the three temperatures examined. Figure 2 summarizes the organization and structural evolution of the TRCDA film at 5 °C. The surface pressure−area isotherm of TRCDA at 5 °C on water subphase (Figure 2A) indicates that domains of condensed TRCDA monolayer spontaneously form at zero surface pressure with a limiting molecular area of 26 Å^2 molecule^{-1}. The condensed domains are brought together by the compression, followed by a collapse of the monolayer, which occurs at around 13 mN/m. At that point, the TRCDA undergoes transformation into a trilayer film (at higher pressures) as indicated by the limiting molecular area of approximately 9 Å.[2,11]

The BAM images provide a microscopic textural description of the compression process. Initially, condensed TRCDA monolayer plates appear (Figure 2Bi), which rapidly populate the entire film surface as the pressure increases (Figure 2Bii). At the collapse pressure around 13 mN/m, small trilayer[11,19] domains appear as white regions in the BAM image (Figure 2Biii); the increased brightness is probably due to the greater thickness of the reflecting domains. As the film is compressed further, the white trilayer structures become the dominant feature within the films (Figure 2Biv−v). The BAM data are consistent with the AFM analysis, which suggested that further compression beyond the collapse point induces formation of TRCDA multilayers.[11]

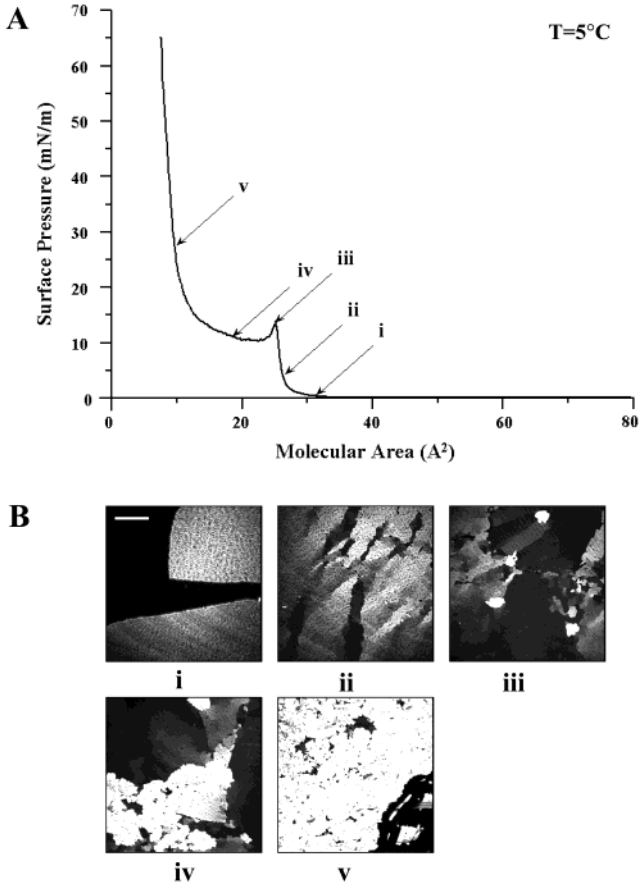

Figure 2. Surface pressure−area isotherm (A) of TRCDA film at 5 °C and (B) BAM images recorded at the indicated points within the isotherm. The bar represents 100 μm.

Different structural features are observed when the TRCDA film is compressed at 18 °C, Figure 3. In contrast to the surface pressure−area isotherm at 5 °C, the isotherm of TRCDA acquired at 18 °C, Figure 3A, features an initial liquid expanded phase, which transforms into a condensed monolayer at a surface pressure of 5 mN/m. The monolayer further collapses at around 10 mN/m, followed by coexisting monolayer and trilayer phases.[11] The BAM results provide a striking visual insight into the development of the film structures at 18 °C. Figure 3Bi, in particular, shows the TRCDA monolayer, apparent as the growing dendritic "feathers", coexisting with the liquid expanded phase, essentially the dark background corresponding to the relatively low density of the expanded liquid monolayer. This image is in full agreement with the isotherm indicating the existence of equilibrium between the expanded and condensed TRCDA phases.

The appearance of dendritic growth of the TRCDA monolayer in Figure 3Bi is significant and sheds light on the mechanism of film organization. Branched, dendritic patterns in interfacial growth are usually a consequence of nonequilibrium conditions at the growth interface.[20,21] Formation of similar patterns was observed in compressed monolayers during a first-order liquid expanded−liquid condensed phase transition at a high compression rate[22,24] or during monolayer compression near a critical temperature.[25,26] The dendritic patterns point to diffusion-limited aggregation (DLA)[27] as the most likely mechanism corresponding to the formation of the TRCDA monolayer. The DLA model, which assumes an immobile cluster progressively growing by aggregation of monomer particles with a sticking probability of a unity, has been successfully applied to describe fractal aggregation phenomena in various systems.[28,29]

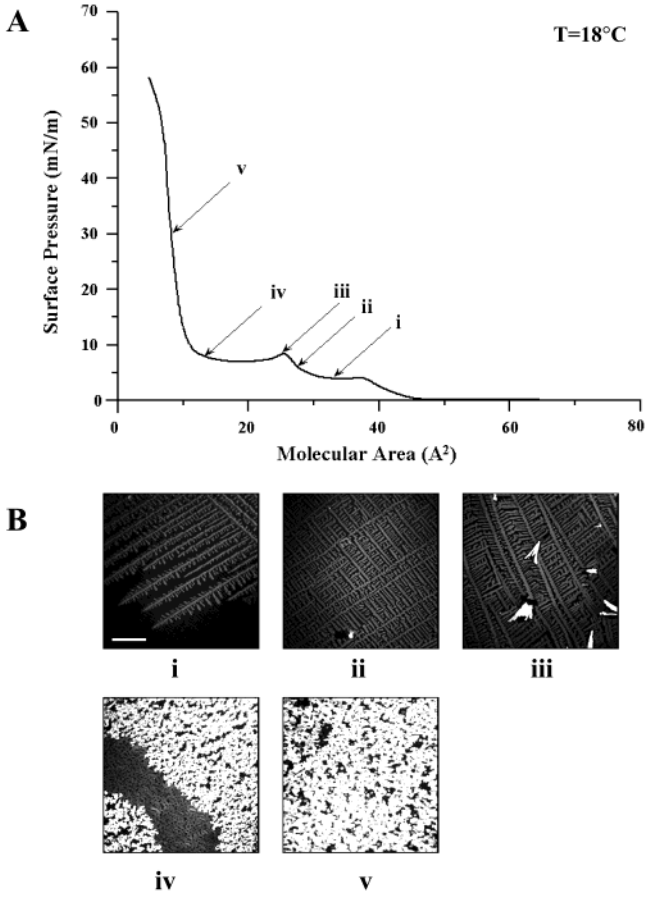

Figure 3. Surface pressure−area isotherm (A) of TRCDA film at 18 °C and (B) BAM images recorded at the indicated points within the isotherm. The bar represents 100 μm.

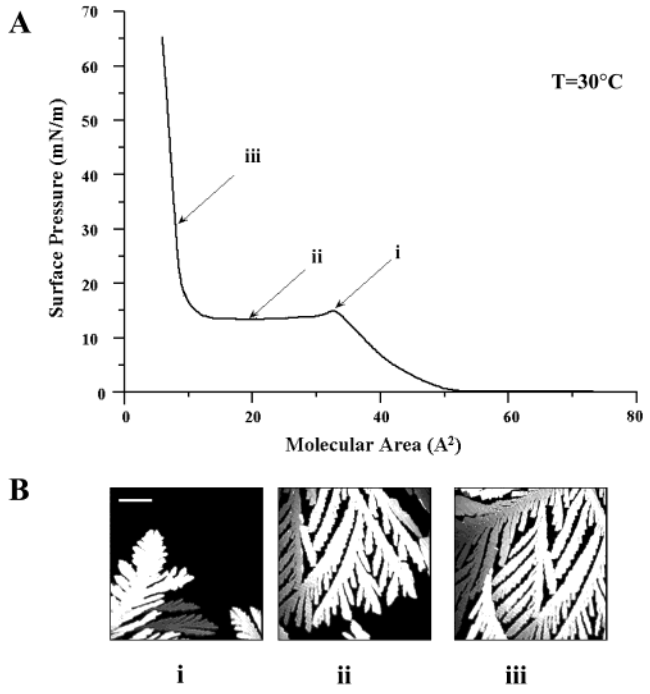

Figure 4. Surface pressure−area isotherm (A) of TRCDA film at 30 °C and (B) BAM images recorded at the indicated points within the isotherm. The bar represents 100 μm.

In the case of the TRCDA film, the experimental conditions are somewhat different compared with the classical DLA configuration of Witten and Sander.[30] Specifically, the surface

pressure−area isotherms in this study are measured by progressively reducing the molecular area. This condition implies that the molecular domains grow with velocity compression, which influences the growth process as the two-dimensional area decreases. Furthermore, unlike the DLA model which assumes random shapes, the order and symmetry of the TRCDA domains are determined to a large extent by the crystallization processes occurring within the diacetylene monolayer. A previous study employing a Monte Carlo simulation, which assumed an aggregation growth of a two-dimensional square lattice, attempted to reproduce the conditions of the surface pressure−area measurements.[31] That analysis has confirmed that the growth process of a condensed monolayer phase gives rise to dendrite formation, limited by the free diffusion of particles in the expanded phase. Furthermore, following compression, the dendritic structures are expected to disappear through transformation into denser structures.[31] Intriguingly, stopping the compression at surface pressures in which fractal-dendritic structures appear (Figure 3B) resulted in slow modification of the dendritic morphology, further supporting the nonequilibrium nature of this growth phenomenon.

Particularly interesting is the striking difference between the morphologies of the condensed TRCDA monolayer at 5 and 18 °C. The images acquired at 5 °C (e.g., Figure 2Bi−ii) and 18 °C (Figure 3Bi−ii) point to a significantly denser distribution of the bright TRCDA monolayer domains at 5 °C. This observation is most likely due to the stabilization of closer monolayer packing by lower temperatures, which is similarly apparent by the limiting molecular areas of the collapse points in 26 Å^2 at 5 °C (Figure 2A) and 30 Å^2 at 18 °C (Figure 3A). The increase of the surface pressure in which the expanded phase−condensed phase transition occurs, at higher temperatures, is attributed to higher Brownian motion, which stabilizes the expanded phase. Similarly, the denser monolayer observed at 5 °C, compared to the monolayer at 18 °C, is ascribed to the less-pronounced molecular motion within the domain interface at lower temperatures, as well as the rather general observation of denser two-dimensional and three-dimensional structures at lower temperatures.

Distinct textural features are recorded when the TRCDA film is compressed at 30 °C, Figure 4. The surface pressure−area isotherm shown in Figure 4A indicates that the higher temperature in effect causes disappearance of the condensed phase and increases the stability of the expanded phase. Indeed, no organized monolayers appear in the BAM images, Figure 4B, prior to the collapse point, denoted i, in the isotherm (Figure 4A). The BAM data provide dramatic visualization of the direct transition between the expanded phase (the dark background) and the nonequilibrated trilayer film, which grows in a fractal-like manner. The observation of fractal branching in Figure 4 suggests that even the transition of TRCDA from an expanded phase directly into the multilayer structure is governed by anisotropic growth, similar to that observed in the case of the condensed monolayer (Figures 2 and 3). Moreover, the branching seems to occur randomly but rather predominantly to one direction within a branch.

One of the most important questions that we address in this study is the effect of the embedded lipid molecules upon the structural properties of mixed lipid/PDA films. These films are used as a two-dimensional model for the colorimetric liposome assemblies employed as biosensors for various membrane processes.[5,8] Our previous work has explored the incorporation of phosphatydilcholine [PC] into TRCDA films and the thermodynamic modification induced by the lipids.[11] In particular, addition of the phospholipids has been shown to both stabilize the expanded phase of the films and increase the pressure in which the expanded−condensed phase transition occurs.[11] Figure 5 provides further insight into the relationship between the temperature and structural properties of a mixed DMPC/TRCDA (1:4 molar ratio) film deposited on pure water subphase.

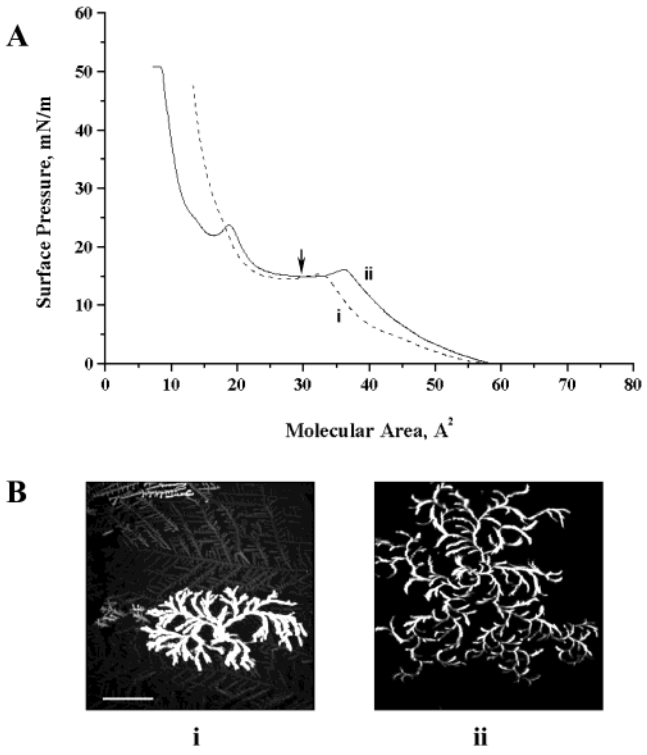

Figure 5. Surface pressure−area isotherms (A) of DMPC/TRCDA (1:4 molar ratio) recorded at (i) 15 and (ii) 18 °C and (B) BAM images recorded at the indicated points within the isotherm. The bar represents 100 μm.

Figure 5A depicts the surface pressure−area isotherms of the DMPC/TRCDA film at 15 and 18 °C. The isotherms clearly indicate that incorporation of the phospholipids stabilizes the expanded phase. While at 15 °C the isotherm i exhibits a shoulder indicative of a transition between the expanded phase and condensed monolayer, at 18 °C (isotherm ii) the film seems to undergo a direct transformation from an expanded liquid into a multilayer organization. Moreover, the collapse point observed at 18 °C at around 15 mN/m is higher than the corresponding point recorded for a pure TRCDA film, Figure 3, which is similarly related to the stabilization effect of the embedded lipid molecules.

The BAM images in Figure 5B, taken at the plateau regions of the isotherms, further illuminate the organization of the TRCDA domains in the mixed film. Specifically, while at 15 °C (Figure 5Bi) the film exhibits both a condensed phase (the pale dendritic regions) and the branched multilayer structures (bright domains), at 18 °C no condensed TRCDA monolayer is detected (Figure 5Bii). This is similarly manifested as the shallow shoulder in isotherm i around 40 Å^2 molecule^{-1}, which is due to the transition from the liquid expanded phase (background) to the condensed, pale dendritic background.

The BAM images thus confirm the presence of a condensed monolayer TRCDA phase at 15 °C and its elimination at the higher temperature. A noteworthy observation is the relatively less ordering apparent in the TRCDA monolayer in the mixed DMPC/TRCDA film (Figure 5Bi) compared to pure TRCDA

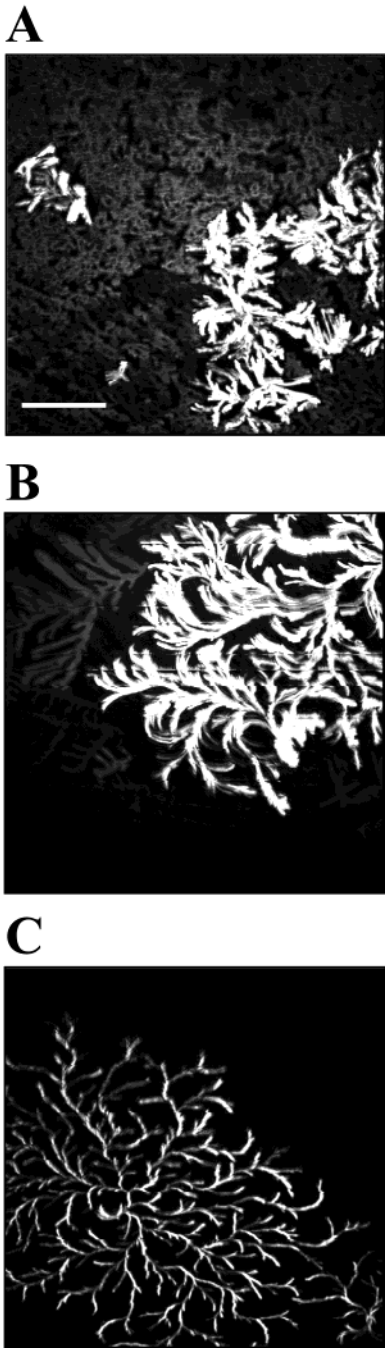

Figure 6. BAM images of DMPC/TRCDA films recorded at the collapse point at molecular areas of approximately 30 Å^2 at 18 °C. The molar fractions of DMPC in the mixed films were (A) 5%, (B) 10%, and (C) 20%. The bar represents 100 μm.

(Figure 3Bi,ii). The less-organized monolayer structure suggests that there is a distinct effect of the incorporated lipids upon the growth process of the diacetylene acid. Particularly interesting in Figure 5Bii is the appearance of the curved morphology of the TRCDA multilayers. This result is a further evidence that the phospholipids affect the structure and organization of the TRCDA matrix and that the interface between the two molecular assemblies plays an active role in determining the film properties.

Further insight into the effect of incorporated phospholipids upon the aggregation properties of compressed TRCDA films is provided in Figure 6, which presents BAM images recorded at 18 °C for films with different lipid/diacetylene molar ratios. Significantly, the BAM images were all acquired immediately

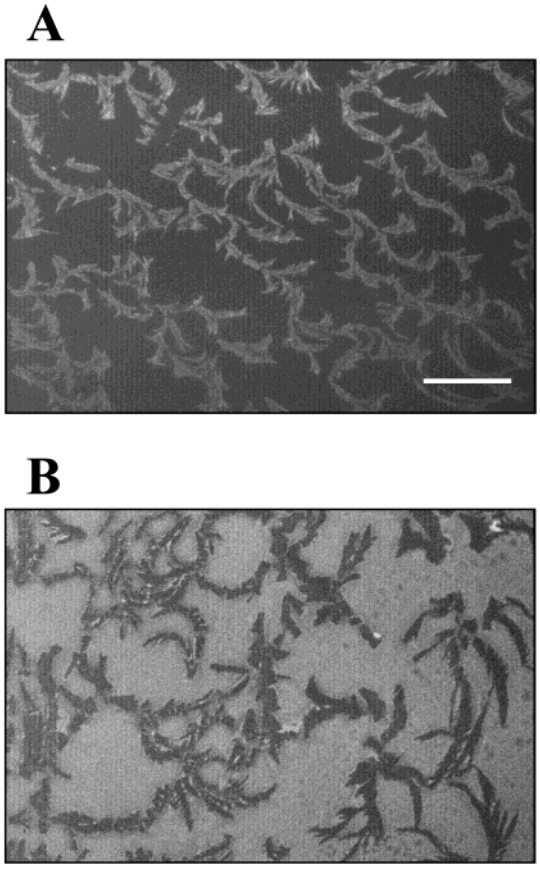

Figure 7. Fluorescent images of polymerized DMPC/TRCDA (30% DMPC molar fraction) films compressed to 30 mN/m and transferred to OTS-modified glass slides: (A) fluorescent red-phase TRCDA recorded at 520 nm; (B) DMPC/TRCDA film doped with the fluorescent probe NBD-PE, see text. The bar represents 10 μm.

following the first collapse point in the respective isotherms (Figure 5)—at the transition from the expanded phase to the condensed/multilayer phases. The BAM data clearly indicate that when the percentage of the phospholipids in the film is low (under 20%, Figure 6A,B), condensed TRCDA monolayers are formed, shown as the low-intensity features in the images. However, when the phospholipid content in the film becomes relatively high (30%, Figure 6C), the monolayer phase does not appear any more because of stabilization of the expanded phase by the phospholipids.[11] Inspection of the pictures shown in Figure 6 further reveals that increasing the concentration of phospholipids in the films gives rise to more curved morphologies of the TRCDA domains. Furthermore, the apparent "thinning" of the TRCDA domains shown in Figure 6C is consistent with the reduction of the polymer domain size, previously observed by atomic force microscopy in mixed DMPC/TRCDA films.[11] These results are consistent with the data presented in Figure 5 and further suggest that interfacial interactions between the lipids and TRCDA play a significant role in the growth processes.

The BAM experiments, summarized in Figures 2−6, provide a wealth of structural and textural information on the organization and growth properties of the TRCDA domains. Fluorescence microscopy has been additionally applied to corroborate the BAM analysis and, in particular, to examine the effect of film polymerization. Furthermore, the fluorescence experiments have been designed to obtain a better insight into the distribution of the phospholipid molecules in the mixed films, Figure 7. Figure 7A shows the fluorescence microscopy image of UV-irradiated DMPC/TRCDA film at 18 °C. The bright regions in

Figure 7A correspond to the polymerized "red-phase" TRCDA domains, which fluoresce at around 530 nm, while the nonfluorescent phospholipid molecules are located within the dark background. The fluorescence image in Figure 7A highly resembles the BAM results (Figures 3 and 5), and it indicates that polymerization of the film does not affect the distribution and organization of the polymer matrix.

The fluorescence microscopy image in Figure 7A confirms that the lipids and polymer are segregated within the DMPC/TRCDA film. Supporting that conclusion is the picture shown in Figure 7B, depicting polymerized DMPC/TRCDA film at 18 °C doped with the fluorescent marker NBD-PE. NBD-PE molecules, which are miscible within phospholipid assemblies but not within the condensed diacetylene regions, have been extensively used for studying lipid interfaces.[31,32] Examination of the fluorescence result in Figure 7B shows that the distribution of dark and bright regions within the film is essentially reversed compared to the image shown in Figure 7A. This result is important because it confirms that the fluorescent dye both is miscible exclusively within the expanded-phase phospholipid regions and is not significantly incorporated within the more organized TRCDA domains. Furthermore, it confirms the BAM data indicating that segregation between the lipid and polymer moieties occurs during compression of the film.

The fluorescence images in Figure 7 indicate that the domain sizes of polymerized TRCDA appear smaller compared to the nonpolymerized film (Figure 5). This is mostly related to the relatively high percentage of lipid in the film (30%) and the high surface pressure in which the films were transferred to the glass substrate. Importantly, however, the fluorescence microscopy experiment shows that the fractal organization of TRCDA and the exclusion of the lipid molecules from the polymer domains are independent of the actual polymerization. Moreover, transfer of the polymerized film onto the hydrophobic glass surface does not seem to affect the organization of the film components. This result points to the potential utilization of surface techniques such as atomic force microscopy [AFM] for characterization of film structures and properties.[11]

Conclusions

The structural features, organization, and growth properties of TRCDA and DMPC/TRCDA films have been studied using a combined thermodynamic and microscopic analysis. BAM and fluorescence microscopy experiments have allowed visualization of the progression of TRCDA domain growth and the effect of the incorporated phospholipids upon the film morphology.

The BAM results indicate that the condensed monolayer phase of TRCDA adopts a dendritic structure and that diffusion-limited aggregation is most likely a primary factor in determining the growth morphology of the TRCDA domains. Furthermore, even after film collapse, the TRCDA multilayers similarly exhibit branched fractal structures, of which the appearance depends on the compression temperature.

The microscopic analysis had shed light upon the effects of inclusion of phospholipids on the compression properties and structural features of the films. The BAM images have confirmed that DMPC molecules included in the film enhance the stability of the expanded TRCDA phase and at high DMPC/TRCDA molar ratios the condensed TRCDA monolayer disappears altogether. Intriguingly, the microscopy experiments reveal that increasing the phospholipid concentration within the Langmuir films also significantly affects the morphology the TRCDA domains, specifically through increased bending of the observed structures.

The microscopic study described here is important for potential utilization of lipid/TRCDA films as chemical and biological sensors. The apparent segregation and interfacial contact between the lipid and polymer domains should allow the polymerized domains to act as an actual colorimetric reporter for molecular processes occurring exclusively within the lipid domains, which mimic biological membranes. Furthermore, the dependence of domain size and morphologies upon externally controlled parameters, such as temperature, surface pressure, and film composition, would allow fine-tuning of the sensing capabilities of the film assemblies.

In conclusion, this study provides an important insight into the organization and interfacial properties of TRCDA-based films. The microscopic analysis has contributed to a better understanding of the mixing properties of phospholipid/TRCDA systems and the parameters affecting the morphology and growth of the diacetylene lipid domains. This work would assist in understanding and utilizing the unique chromatic and biosensing properties of lipid/polydiacetylene supramolecular assemblies.

Acknowledgment. R.J. is grateful to the Israel Science Foundation for financial support.

References and Notes

(1) Wegner, G. *Z. Naturforsch*. **1969**, *24B*, 824.
(2) Sugi, M. J. *Mol. Electron*. **1985**, *1*, 3.
(3) Khanarian, G. *Thin Solid Films* **1987**, *152*, 265.
(4) Cheng, Q.; Stevens, R. C. *Adv. Mater*. **1997**, *9*, 481.
(5) Kolusheva, S.; Boyer, L.; Jelinek, R. *Nature Biotech*. **2000**, *18*, 225.
(6) Kolusheva, S.; Shahal, T.; Jelinek, R. *J. Am. Chem. Soc*. **2000**, *122*, 776.
(7) Kolusheva, S.; Kafri, R.; Katz, M.; Jelinek, R. *J. Am. Chem. Soc*. **2001**, *123*, 417.
(8) Evrard, D.; Touitou, E.; Kolusheva, S.; Fishov, Y.; Jelinek, R. *Pharm. Res*. **2001**, *18* (7), 943−949.
(9) Jelinek, R.; Kolusheva, S. *Biotechnol. Adv*. **2001**, *19* (2), 109−118.
(10) Okada, S.; Peng, S.; Spevak, W.; Charych, D. *Acc. Chem. Res*. **1998**, *31*, 229.
(11) Gaboriaud, F.; Golan, R.; Volinsky, R.; Berman, A.; Jelinek, R. *Langmuir* **2001**, *17*, 3651−3657.
(12) Hönig, D.; Möbius, D. *J. Phys. Chem*. **1991**, *95*, 4590−4592.
(13) Henon, S.; Meunier, J. *Rev. Sci. Instrum*. **1991**, *62*, 936−939.
(14) Wang, S.; Lunn, R.; Krafft, M.; Leblanc, R M. *Langmuir* **2000**, *16* (6), 2882−2886.
(15) Wang, S.; Ramirez, J.; Chen, Y.; Wang, P. G.; Leblanc, R. M. *Langmuir* **1999**, *15*, 5623.
(16) Gaines, G. L., Jr. *Insoluble Monolayers at Liquid−Gas Interfaces*; Wiley-Interscience: New York, 1966.
(17) Tscharner, V.; McConell, H. M. *Biophys. J*. **1981**, *36*, 421−427.
(18) Petty, M. C. *Langmuir−Blodgett Films. An Introduction*; Cambridge University Press: Cambridge, U.K., 1996.
(19) Lio, A.; Reichert, A.; Dong, J. A.; Nagy, J. O.; Salmeron, M.; Charych, D. H. *Langmuir* **1997**, *13*, 6524.
(20) Ben-Jacob, E.; Garik, P. *Nature* **1990**, *343*, 523−530.
(21) Gehlert, U.; Vollhardt, D. *Langmuir* **1997**, *13*, 277−282.
(22) Lösche, M.; Möhwald, H. *Eur. Biophys. J*. **1984**, *11*, 35−42.
(23) Knobler, C. M. *Science* **1990**, *249*, 870−874.
(24) Weidemann, G.; Vollhardt, D. *Biophys. J*. **1996**, *70*, 2758−2766.
(25) Suresh, K. A.; Nittmann, J.; Rondelez, F. *Europhys. Lett*. **1988**, *6*, 437−443.
(26) Weideman, G.; Vollhardt, D. *Langmuir* **1997**, *13*, 1623−1628.
(27) Witten, T. A., Jr.; Sander, L. M. *Phys. Rev. Lett*. **1981**, *47*, 1400−1403.
(28) Vicsek, T. *Fractal Growth Phenomena*, 2nd ed., World Scientific: Singapore, 1992.
(29) Barabasi, A.-L.; Stanley, H. E. *Fractal concepts in surface growth*; Cambridge University Press: Cambridge, U.K., 1995.
(30) Witten, T. A., Jr.; Sander, L. M. *Phys. Rev. B* **1983**, *27*, 5686−5697.
(31) Uwaha, M.; Saito, Y. *Phys. Rev. A* **1989**, *40*, 4716.
(32) McConlogue, C.; Vanderlick, T. *Langmuir* **1997**, *13*, 7158−7164.
(33) Park, C. K.; Schmitt, F. J.; Evert, L.; Schwartz, D. K.; Israelachvili, J. N.; Knobler, C. M. *Langmuir* **1999**, *15*, 202−206.